

---

# Online Learning in Contextual Bandits using Gated Linear Networks

---

Eren Sezener<sup>1\*</sup> Marcus Hutter<sup>1\*</sup> David Budden<sup>1</sup> Jianan Wang<sup>1</sup> Joel Veness<sup>1</sup>

## Abstract

We introduce a new and completely online contextual bandit algorithm called Gated Linear Contextual Bandits (GLCB). This algorithm is based on Gated Linear Networks (GLNs), a recently introduced deep learning architecture with properties well-suited to the online setting. Leveraging data-dependent gating properties of the GLN we are able to estimate prediction uncertainty with effectively zero algorithmic overhead. We empirically evaluate GLCB compared to 9 state-of-the-art algorithms that leverage deep neural networks, on a standard benchmark suite of discrete and continuous contextual bandit problems. GLCB obtains median first-place despite being the only online method, and we further support these results with a theoretical study of its convergence properties.

## 1. Introduction

The contextual bandit setting has been a focus of much recent attention, benefiting from both being sufficiently constrained as to be theoretically tractable, yet broad enough to capture many different types of real world applications such as recommendation systems. The linear contextual bandit problem in particular has been subject to intense theoretical investigation; the recent book by [Lattimore & Szepesvri \(2020\)](#) gives a comprehensive overview. This line of investigation has yielded principled online algorithms such a LINUCB ([Li et al., 2010](#)), that work well given informative features. To work around the limitations of linear representations in more difficult problems, these algorithms are often used in combination with an offline nonlinear feature extraction technique such as deep learning. A limitation with such approaches is that the feature extraction component is treated as a black box, which runs the risk of ignoring the uncertainty introduced by the offline feature extraction component.

Recent advances in posterior approximation for deep networks has led to the introduction of a variety of approximate Thompson Sampling based contextual bandits algorithms

that perform well in practice. A reoccurring theme across these works is to leverage some kind of efficiently approximated surrogate notion of the estimation accuracy to drive exploration. Noteworthy examples include the use of random value functions ([Osband et al., 2016; 2018](#)), Bayes by Backprop ([Blundell et al., 2015](#)), and noise injection ([Plappert et al., 2018](#)). An empirical comparison of neural network based Bayesian methods can be found in ([Riquelme et al., 2018](#)). A major drawback of these methods is that they are not online, and often require expensive retraining at regular intervals.

Another line of investigation has focused on using count-based approaches to drive exploration via the optimism in the face of uncertainty principle. Here various types of confidence bounds on action value estimates are obtained directly from the state/context-action visitation counts, with algorithms typically choosing an action greedily with respect to the upper confidence bound. Count-based methods have seen noteworthy success in finite armed bandit problems ([Auer et al., 2002](#)), tabular reinforcement learning ([Strehl & Littman, 2008; Lattimore & Hutter, 2014](#))), planning in MDPs ([Kocsis & Szepesvári, 2006](#)), amongst others. For the most part however, the usage of count based approaches has been limited to low dimensional settings, as counts get exponentially sparser as the state/context-action dimension increases. As a remedy to this problem, [Bellemare et al. \(2016\)](#) proposed a notion of “pseudocounts”, which utilize density-like approximations to generalize counts across high-dimensional states/contexts. Impressive performance was obtained in popular reinforcement learning settings such as Atari game playing when using this technique to drive exploration. Another approach which pursued the idea of generalizing counts to higher dimensional state spaces was the work of [Tang et al. \(2017\)](#), who proposed an elegant approach that used the SimHash ([Charikar, 2002](#)) variant of locality-sensitivity hashing to map the original state space to a smaller space for which counting state-visitation is tractable. This approach led to strong results in both Atari and continuous control reinforcement learning tasks.

In this work, we introduce a new online contextual bandit algorithm that combines the benefits of scalable non-linear action-value estimation with a notion of hash based pseudocounts. For action-value estimation we use a Gated Linear Network (GLN) that employs half-space gating, which has

---

\*Equal contribution <sup>1</sup>DeepMind. Correspondence to: Eren Sezener <esezener@google.com>.

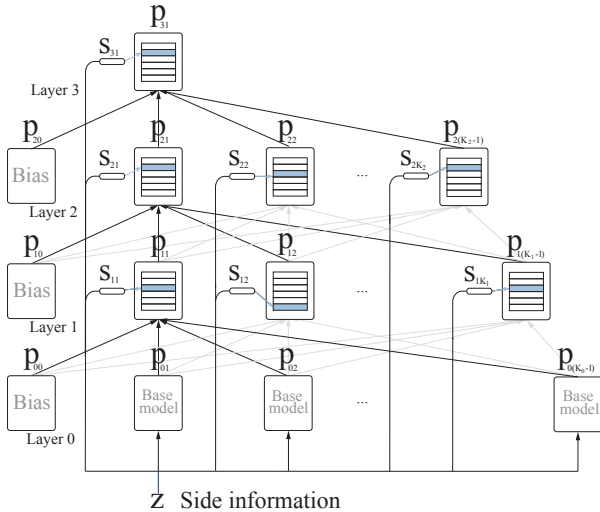


Figure 1. A graphical depiction of a Gated Linear Network. Each neuron receives inputs from the previous layer as well as the broadcasted side information  $z$ . The side information is passed through all the gating functions, whose outputs  $s_{ij} = c_{ij}(z)$  determine the active weight vectors (shown in blue).

recently been shown to give rise to universal function approximation capabilities (Veness et al., 2019; 2017). To drive exploration, our key insight is to exploit the close connection between half-space gating and the SimHash variant of locality-sensitivity hashing; by associating a counter to each neurons gated weight vector, we can define a pseudocount based exploration mechanism that can generalise in a way similar to the work of Tang et al. (2017), with essentially no additional computational overhead beyond obtaining a GLN based action-value estimate. Furthermore, since the gating in a GLN is directly responsible for determining its inductive bias, our notion of pseudocount is tightly coupled to the networks parameter uncertainty, which allows us to naturally define a UCB-like (Auer et al., 2002) policy as a function the pseudocounts. We demonstrate the empirical efficacy of our method across a set of real-world and synthetic datasets, where we show that our policy outperforms all of the state-of-the-art neural Bayesian methods considered in the recent survey of Riquelme et al. (2018) in terms of median/mean rank.

## 2. Background

In this section we give a short overview of Gated Linear Networks sufficient for understanding the contents of this paper. We refer the reader to reader to (Veness et al., 2017; 2019) for additional background.

**Gated Linear Networks.** (GLNs) (Veness et al., 2017) are feed-forward networks composed of many layers of gated geometric mixing neurons; see Figure 1 for a graphi-

cal depiction. Each neuron in a given layer outputs a gated geometric mixture of the predictions from the previous layer, with the final layer consisting of just a single neuron that determines the output of the entire network. In contrast to an MLP, the side information (or input features) are broadcast to every single neuron, as this is what each gating function will operate on. The distinguishing properties of this architecture are that the gating functions are fixed in advance, each neuron attempts to predict the same target with an associated per-neuron loss, and that all learning takes place locally within each neuron.

**Gated Geometric Mixing.** We now give a brief overview of gated geometric mixing neurons, and describe how they learn; a comprehensive description can be found in Section 2 in the work of Veness et al. (2017).

Geometric Mixing is a simple and well studied ensemble technique for combining probabilistic forecasts. It has seen extensive application in statistical data compression (Mattern, 2012; 2013). One can think of it as a parametrised form of geometric averaging, or as a product of experts (Hinton, 2002). Given  $p_1, p_2, \dots, p_d$  input probabilities predicting the occurrence of a single binary event, geometric mixing computes  $\sigma(w^\top \sigma^{-1}(p))$ , where  $\sigma(x) := 1/(1 + e^{-x})$  denotes the sigmoid function,  $\sigma^{-1}$  its inverse – the logit function,  $p := (p_1, \dots, p_d)$  and  $w \in \mathbb{R}^d$  is the weight vector which controls the relative importance of the input forecasts.

A gated geometric mixing neuron is the combination of a gating procedure and geometric mixing. In this work, gating has the intuitive meaning of mapping particular input examples to a particular choice of weight vector for use with geometric mixing. We can represent each neuron’s gated weights by a matrix, with each row corresponding to the weight vector selected by the gating procedure. More formally, associated to every gated geometric mixing neuron will be a gating function  $g : \mathcal{Z} \rightarrow \mathcal{S}$ ,  $\mathcal{S} = \{1, \dots, S\}$  for some integer  $S > 1$ , where  $\mathcal{Z}$  denotes the space of possible side information and  $\mathcal{S}$  denotes the signature for each weight vector. The weight matrix can now be defined as  $W = (w_1, \dots, w_s)^\top \in \mathcal{W}$ , where  $\mathcal{W}$  is assumed to be a convex set  $\mathcal{W} \subset \mathbb{R}^{s \times d}$ . The key idea is that such a neuron can specialize its weighting of the input predictions based on some neuron-specific property of the side information  $z$ .

Online learning under the logarithmic loss can be realized in a principled and efficient fashion using Online Gradient Descent (Zinkevich, 2003), as the loss function

$$\ell(z, p | W) := -\log(\sigma(W_{g(z)*} \cdot \sigma^{-1}(p))) \quad (1)$$

is a convex function of the active weights  $W_{g(z)*} \equiv w_{g(z)}^\top$ . By forcing  $\mathcal{W}$  to be a (scaled) hypercube, the projection step can be implemented efficiently using clipping.

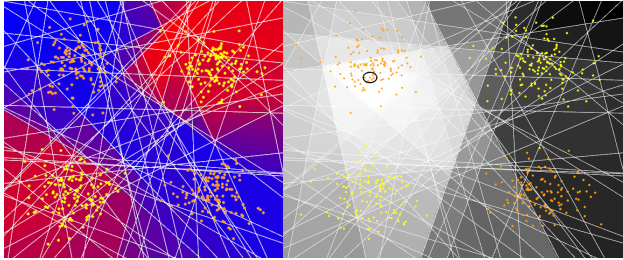


Figure 2. (Left) The learnt decision boundary after a single pass through the 2D Noisy XOR dataset. The white lines show the boundaries between the halfspaces defining the gates of a GLN overlaid, which shows the division of a 2D input space into many convex polytopes. Each point falling within a particular convex polytope is a function of the same underlying learnt multilinear polynomial. (Right) The intensity of the white shading indicates the change in decision boundary of training on a single point (indicated by a black circle) of an untrained GLN.

**Networks of Gated Geometric Mixers.** We now return to more concretely describing the network architecture depicted in Figure 1. Upon receiving an input, all the gates in the network fire, which corresponds to selecting a single weight vector local to each neuron from the provided side information for subsequent use with geometric mixing. It is important to note that such networks are *data-dependent* piecewise linear networks, as each neuron’s input non-linearity (the logit function) is inverse to the output non-linearity (the sigmoid function).

Returning to Figure 1, each rounded rectangle depicts a Gated Geometric Mixing neuron; the bias is a scalar value between 0 and 1. There are two types of input to each neuron: the first is the side information  $z$ , which can be thought of as the input features in a standard supervised learning setup; the second is the input to the neuron, which will be the predictions output by the previous layer, or in the case of layer 0, some function of the side information. The side information is fed into every neuron via the context function  $g_{ij} : \mathcal{Z} \rightarrow \mathcal{S}_{ij}$  for neuron  $j$  in layer  $i$  to determine which weight vector  $w_{ijg_{ij}(z)}$  is active in matrix  $w_{ij}$  for a given input. Each neuron attempts to directly predict the target, and these predictions are fed into higher layers. The loss function associated with each neuron is given by Eq.(1) applied to  $w_{ij}$  using its respective gating function  $g_{ij}$ . It is important to note that both prediction and weight update require just a single forward computational pass of the network, as one can see from inspecting Algorithm 1.

**Random Halfspace Gating** The choice of GLN gating function (i.e.,  $g_{ij}$ ) is paramount, as it determines the inductive bias and capacity of the network. Here we restrict our attention to halfspace gating, which was shown in (Veness et al., 2017) to be universal in the sense that sufficiently large halfspace gated GLNs can model any bounded, con-

tinuous and compactly supported density function by only *locally optimizing* the loss at each neuron.

Given a finite sized halfspace GLN, we need a mechanism to select the fixed gates for each neuron. Promising initial results were shown in (Veness et al., 2017) for simple classification problems when the normal vector of each halfspace was sampled i.i.d. from Gaussian distribution. Here we add some intuition about the learning dynamics which will motivate our subsequent exploration heuristic.

In (Veness et al., 2017) it was shown that one can rewrite the output of an  $L$ -layer GLN, with  $K_i$  neurons in layer  $i$ , and with input  $p_0$  and side information  $z$ , as

$$\text{GLN}(p_0, z) = \sigma \left( \underbrace{W_L(z) W_{L-1}(z) \dots W_1(z)}_{\text{multilinear polynomial in } z \text{ of degree } L} \text{logit}(p_0) \right).$$

where each matrix  $W_i(z)$  is of dimension  $K_i \times K_{i-1}$ , with each row constituting the active weights (as determined by the gating) for the  $j$ th neuron in layer  $i$ . Here one can see that the product of matrices collapses to a multilinear polynomial in the learnt weights; an example of this is shown in Figure 2 (Left). Note that the resulting multilinear polynomial may be different for different  $z$ , resulting in a much richer class of models. Thus the depth and shape of the network influences how the GLN will generalize. Figure 2 (Right) shows the effects on the change in decision boundary of training on a single data point. The magnitude of the change is largest within the convex polytope containing the training point, and decays with respect to the remaining convex polytopes according to how many halfspaces they share with the containing convex polytope. This makes intuitive sense, as since the weight update is local, each row of  $W_i(z)$  is pushed in the direction to better explain the data independently of each other. One can think of a GLN as a kind of smoothing technique – input points which cause similar gating activation patterns must have similar outputs.

This observation motivated the following heuristic idea for exploration: if we associated a counter with every halfspace, which was incremented whenever we updated the weights there whenever we see a new data point, and simply summed the counts of all its active halfspaces, we would get a good sense as to how well we would expect the GLN to generalize within this region. This intuition is the basis for the algorithms we explore in Section 3.

**Prediction and Weight Update.** Both prediction and online learning using Online Gradient Descent can be implemented in a single forward pass of the network. We will define this forward pass as helper routine in Algorithm 1, and in subsequent sections instantiate it to compute various quantities of interest for our contextual bandit application.

We will use notation consistent with Figure 1. Layer 0 will correspond to the input features. Here  $K_i \in \mathbb{N}$  de-

**Algorithm 1** GLN( $\Theta, z, x, r, \eta$ , update).

Perform a forward pass and optionally update weights. Each layer performs clipped geometric mixing over the outputs of the previous layer, where the mixing weights are side-info-dependent via the gating function (Line 10). Lines 12-13 apply (optionally) the weight update, which is obtained by differentiating the per neuron local loss (Veness et al., 2017, Prop.1).

```

1: Input: GLN weights  $\Theta \equiv \{w_{ijs}\}$ 
2: Input: side info  $z$ , base predictions  $x \in [\epsilon; 1 - \epsilon]^{K_0-1}$ 
3: Input: binary target  $r$ , learning rate  $\eta \in (0, 1)$ 
4: Input: boolean update (controls if we learn or not)
5: Output: estimate of  $\mathbb{P}[r = 1 | x]$ 

6:  $p_0 \leftarrow (\beta, x_1, x_2, \dots, x_{K_0-1})$ 
7: for  $i \in \{1, \dots, L\}$  do {over layers}
8:    $p_{i0} \leftarrow \beta$ 
9:   for  $j \in \{1, \dots, K_i\}$  do {over neurons}
10:     $p_{ij} \leftarrow \text{CLIP}_{\epsilon}^{1-\epsilon} [\sigma(w_{ijg_{ij}}(z) \cdot \text{logit}(p_{i-1}))]$ 
11:    if update then
12:       $\Delta_{ij} \leftarrow -\eta (p_{ij} - r) \text{logit}(p_{i-1})$ 
13:       $w_{ijg_{ij}} \leftarrow \text{CLIP}_{-b}^b [w_{ijg_{ij}} + \Delta_{ij}]$ 
14:    end if
15:  end for
16: end for
17: return  $p_{L1}$ 
    
```

notes the number of neurons in layer  $i$ , with  $L$  denoting the number of layers excluding the base layer (Layer 0). The prediction made by the  $j$ th neuron in layer  $i$  is denoted by  $p_{ij} \in [\epsilon, 1 - \epsilon]$ , for all  $0 \leq j < K_i$ , for all layers  $0 \leq i \leq L$ . The vector of predictions from all neurons within layer  $i$  is denoted by  $p_i = (p_{i0}, \dots, p_{iK_i-1})$ . The base predictions used for the first layer need to lie within  $[\epsilon, 1 - \epsilon]$  to satisfy the constraints imposed by geometric mixing; if the contextual side information  $z$  lies outside this range, one would typically define the base prediction  $x := f(z)$ , where  $f$  is some squashing function. Here we adopt the convention that  $p_{i0}$  is a constant bias  $\beta \in [\epsilon, 1 - \epsilon] \setminus \{0.5\}$ . Associated with each neuron is a gating function  $g_{ij}$  that determines which vector of weights to use for any given side information. Note that all neuron predictions are clipped to lie within  $[\epsilon, 1 - \epsilon]$ ; this ensures that the  $\ell_2$  norm of any gradient is finite. We define the prediction clipping function as  $\text{CLIP}_{\epsilon}^{1-\epsilon}[x] := \min\{\max(x, \epsilon), 1 - \epsilon\}$ . The weight space for the  $j$ th neuron in layer  $i > 0$  is a convex set  $\mathcal{W}_{ij} \subset \mathbb{R}^{K_{i-1}}$ ; typically one would use the same convex set across all neurons within a single layer, however this is not required. For each neuron  $(i, j)$ , we project its weights after a gradient step onto the convex set  $\mathcal{W}_{ij}$ . In practical implementations one typically would set  $\mathcal{W}_{ij} = [-b, b]^{K_{i-1}}$ , for some constant  $10 < b < 100$ , for all  $j$ . This projection can be implemented efficiently by clipping every component of

$w_{ijs}^{(t)}$  to lie within  $[-b, b]$ . The matrix of *gated* weights for the  $j$ th neuron in layer  $i$  is denoted by  $w_{ij} \in \mathbb{R}^{S_{ij} \times K_{i-1}}$ . We denote by  $\Theta = \{w_{ijs}\}_{ijs}$  the set of all gated weight vectors for the network.

### 3. Gated Linear Contextual Bandits

We now introduce our Gated Linear Contextual Bandits (GLCB) algorithm, a contextual bandit technique that utilizes GLNs for estimating expected rewards of arms and using its associated gating functions to derive exploration bonuses.

Let  $\mathcal{X} \subseteq [0; 1]^{K_0-1}$  be a set of contexts and  $\mathcal{A}$  be a finite set of actions. At each discrete timestep  $t$ , the agent observes a context  $x_t \in \mathcal{X}$  and takes an action  $a_t \in \mathcal{A}$ , receiving a context-action dependent reward  $r_t$ . The goal is to maximize the cumulative rewards  $\sum_{t=1}^T r_t$  over an unknown horizon  $T$ . We first consider the case of Bernoulli bandits, then generalize the setup to bounded continuous rewards.

**Bernoulli distributed rewards.** Assume that the rewards  $r_{xat} \sim \text{Bernoulli}(\theta_{xa})$  are conditional i.i.d., where  $\theta_{xa}$  is a context-action dependent reward probability that is unknown to the agent. We will use a separate GLN to estimate the context dependent reward probability  $\Pr[r = 1 | x, a] = \mathbb{E}[r | x, a] = \theta_{xa}$  for each arm. Across arms, each GLN will share the same set of hyperparameters. This includes the shape of the network, the choice of randomly sampled halfspace gating functions for the contexts, the choice of clipping threshold, and weight space. The weight parameters for each neuron on layer  $i \geq 1$  are initialized to  $1/K_{i-1}$ . In our application, there is no need to make a distinction between the input to the network and the side information, so from here onward we drop this dependence by defining

$$\text{GLN}(x | \Theta) := \text{GLN}(\Theta, x, x, 1, 0, \perp).$$

We use  $\Theta_a^t$  to denote the current set of GLN parameters at time  $t$  for action  $a$ , which is learnt from  $\{(x_\tau, r_\tau) : a_\tau = a, \tau < t\}$  using Algorithm 1 with *update* =  $\top$ . Therefore  $\text{GLN}_a^t(x) := \text{GLN}(x | \Theta_a^t)$  is the estimate of the expected reward for an arm  $a$  given context  $x$  at time  $t$ .

From now on we assume each GLN is composed of  $U$  neurons, which we also call *units*, where we denote the index set of the units as  $\mathcal{U} = \{1, \dots, U\}$  which is bijected to our previous (layer,unit) index set  $\{(i, j) : 1 \leq i \leq L, 0 \leq j < K_i\}$ . Each unit is associated with a gating function  $g_u$  where  $u \in \mathcal{U}$ .

**GLCB Policy.** The GLCB policy/action is defined as

$$a_t := \pi_t(x) := \arg \max_{a \in \mathcal{A}} \text{GLNUB}_a^{\bar{t}}(x_t),$$

$$\text{GLNUB}_a^{\bar{t}}(x_t) := \text{GLN}_a^{\bar{t}}(x_t) + C \sqrt{\frac{\log t}{\widehat{N}_{\bar{t}}(\mathbf{g}(x_t), a)}}$$

where  $\bar{t} := t - 1$ ,  $C \in \mathbb{R}_+$  is a constant that scales the exploration bonus,  $\mathbf{g}(x) = (g_1(x), \dots, g_U(x))$  is the total signature, and  $\widehat{N}_{\bar{t}}(\mathbf{g}(x), a)$  is our GLN pseudocount, which we introduce formally next, generalizing the exact count  $N_{\bar{t}}(x, a)$  found in UCB.

**Pseudocounts for GLNs.** Let  $x_{<t} \equiv (x_1, \dots, x_{\bar{t}})$  be the first  $t - 1$  contexts, and  $a_{<t}$  the sequence of actions  $a_t \in \mathcal{A}$  taken by GLCB. Let

$$N_{\bar{t}}^f(c) := \#\{1 \leq \tau < t : f(x_\tau, a_\tau) = c\}$$

be the number of times some property  $f$  of  $(x, a)$  is  $c$  in the first  $t - 1$  time-steps. We drop the superscript  $f$  whenever it can be inferred from the arguments. To start with, we need to know how often action  $a$  is taken in a context with signature  $s_u$  of unit  $u$ , so define

$$N_{\bar{t}}(s_u, a) := \#\{1 \leq \tau < t : g_u(x_\tau) = s_u \wedge a_\tau = a\}.$$

We also need to count the total (action) signature frequency

$$N_{\bar{t}}(\mathbf{s}, a) := \#\{1 \leq \tau < t : \mathbf{g}(x_\tau) = \mathbf{s} \wedge a_\tau = a\}$$

$$N_{\bar{t}}(\mathbf{s}) := \#\{1 \leq \tau < t : \mathbf{g}(x_\tau) = \mathbf{s}\}$$

where  $\mathbf{s} = (s_1, \dots, s_U) = \mathbf{g}(x) = (g_1(x), \dots, g_U(x))$  is the total signature of  $x$ . We now introduce our notion of pseudocount for context  $x$  and action  $a$  as

$$\widehat{N}_{\bar{t}}(\mathbf{s}, a) := \text{AGG}_{u \in \mathcal{U}} N_{\bar{t}}(s_u, a) \quad (2)$$

where  $\text{AGG} \in \{\text{mean}, \text{min}, \text{median}\}$  is a choice of aggregation function.

Although our use of the term ‘‘pseudocount’’ is inspired by (Bellemare et al., 2016), where it is introduced as a generalization of state counts from tabular to non-tabular reinforcement learning settings, note that our specification differs in that it isn’t derived from a density model. Also, the exploration term we use has an additional  $\sqrt{\log t}$  term in the numerator like UCB1 (Auer et al., 2002), which plays an essential role in allowing us to derive the asymptotic results presented in the next section.

The complete GLCB policy for Bernoulli bandits is given in Algorithm 2. Notice too that the signature computation on line 9 can be reused when evaluating each  $\text{GLN}(x_t | \Theta_a^{\bar{t}})$  term, since each action specific GLN uses the same collection of gating functions.

**Bounded, continuous rewards.** If the rewards are not Bernoulli distributed, but rather bounded and continuous, instead of directly predicting expected rewards, we instead model the reward probability distribution. For this, we utilize a tree-based discretization, which recursively partitions up the reward space up to some finite depth by using a GLN to model the probability of each recursive branch. Modelling a quantized reward/return distribution up to some

**Algorithm 2** GLCB-policy for Bernoulli bandits  
*Signature counts are initialized to zero in Line 6. Pseudocounts are computed from signature  $\mathbf{s}$  in Line 11. The action is chosen by combining the pseudo-count-based exploration bonus with the expected reward in Line 12. GLN parameters and counts are updated in Lines 14-17.*

- 1: **Input:**  $(g_u)_{u=1}^U$ , gating functions.
- 2: **Input:**  $(\Theta_a^0)_{a \in \mathcal{A}}$ , initial GLN parameters
- 3: **Input:** AGG, an aggregation function (e.g., median)
- 4: **Output:** Actions  $a_{1:T}$
- 5: **Output:** Trained GLN parameters  $(\Theta_a^T)_{a \in \mathcal{A}}$
- 6:  $N(\cdot, \cdot) \leftarrow 0$
- 7: **for**  $t \in 1, \dots, T$  **do**
- 8:   Observe context  $x_t$
- 9:   Compute signature  $\mathbf{s} \leftarrow \mathbf{g}(x_t)$
- 10:    $\bar{t} \leftarrow t - 1$
- 11:    $\widehat{N}_{\bar{t}}(\mathbf{s}, a) \leftarrow \text{AGG}_{u \in \mathcal{U}} N_{\bar{t}}(s_u, a)$  for all  $a \in \mathcal{A}$
- 12:    $a_t \leftarrow \arg \max_a \left\{ \text{GLN}(x_t | \Theta_a^{\bar{t}}) + C \sqrt{\frac{\log t}{\widehat{N}_{\bar{t}}(\mathbf{s}, a)}} \right\}$
- 13:   Observe reward  $r_t$  by performing  $a_t$
- 14:    $\Theta_{a_t}^t \leftarrow \text{GLN}(\Theta_{a_t}^{\bar{t}}, x_t, x_t, r_t, \top)$
- 15:    $\Theta_a^t \leftarrow \Theta_a^{\bar{t}}$  for  $a \in \mathcal{A} \setminus \{a_t\}$
- 16:    $N_t(s_u, a_t) \leftarrow N_{\bar{t}}(s_u, a_t) + 1$  for all  $u \in \mathcal{U}$
- 17:    $N_t(\mathbf{s}, a) \leftarrow N_{\bar{t}}(\mathbf{s}, a)$  for all other  $\mathbf{s} \in \mathcal{S}$  and  $u \in \mathcal{U}$
- 18: **end for**

finite accuracy has recently proven successful in a number of recent works in Reinforcement Learning such as (Veness et al., 2015; Bellemare et al., 2017).

Algorithm 3 describes the CTREE algorithm, which we use a separate instances of to estimate the expected context dependent reward for each action. We describe the algorithm for a single action for simplicity. The algorithm operates on a complete binary tree of depth  $D$  that maintains a GLN at each non-leaf node.

We assume that our tree divides the bounded reward range  $[r_{\min}, r_{\max}]$  uniformly into  $2^d$  bins at each level  $d \leq D$ . By labelling left branches of a node by 0, and right branches with a 1, we can associate a unique binary string  $b_{1:d}$  to any single internal ( $d < D$ ) or leaf ( $d = D$ ) node in the tree. The  $d$ th element, when it exists, is denoted as  $b_d$ . The root node is denoted by empty string  $\epsilon$ . All nodes of the tree can thus be represented as  $\mathcal{B}^{\leq D} = \{\epsilon\} \cup \bigcup_{d=1}^D \mathcal{B}^d$  and all non-leaf nodes with  $\mathcal{B}^{<D} \equiv \mathcal{B}^{\leq D-1}$ .

We define a vector  $v$  of dimension  $2^D$ , whose components correspond to the ordered list of midpoints in our discretized range, via

$$v = (r_{\min} + (\text{DEC}(b) + 1/2)(r_{\max} - r_{\min})/2^{D+1})_{b \in \mathcal{B}^D}$$

where DEC converts a binary string to a decimal. This

**Algorithm 3** CTREE, performs regression utilizing a tree-based discetization, where nodes are composed of GLNs.

- 1: **Input:** Vector of precomputed bin midpoints  $v$
- 2: **Input:** Observed context  $x_t$  at time step  $t$
- 3: **Input:** Weights for each GLN,  $(\Theta_b)_{b \in \mathcal{B}^{<D}}$
- 4: **Output:** Estimate of  $\mathbb{E}[r|x]$
- 5: **return**  $\sum_{b \in \mathcal{B}^D} P(b|x_t) v_{\text{DEC}(b)}$

quantity is used by the CTREE algorithm in conjunction with the probability of each possible path down the tree to approximate the context dependent expected reward.

Given a context  $x$ , a tree estimating the value of an action, i.e. the GLN parameters for each non-leaf node of the tree  $(\Theta_b)_{b \in \mathcal{B}^{<D}}$ , the probability of a reward corresponding to a bin specified by  $b_{1:D}$  is given by

$$P(b_{1:D}|x) = \prod_{i=1}^D \left| 1 - b_i - \text{GLN}(x | \Theta_{b_{<i}}) \right|.$$

Then, we can obtain the expected reward of an action given a context by weighting each bin midpoint with its corresponding probability, that is  $\sum_{b \in \mathcal{B}^D} P(b|x_t) v_b$ .

Whenever a reward  $r$  is observed, all the GLNs along the path  $b$  to reach the target bin are updated with a target 0 or 1 depending on if it requires traversing left or right to reach the bin containing  $r$ , i.e.  $b$  is the first  $D$  digits of the binary expansion of  $r/(r_{\max} - r_{\min})$ .

We can adapt Algorithm 2 we proposed for Bernoulli bandit problems to bounded-continuous bandit problems by (I) estimating expected rewards  $\mathbb{E}[r|x, a]$  utilizing CTREE's (rather than using a single GLN per action) and (II) aggregating counts across all gating units of  $2^D - 1$  many GLNs for each action. We should note that even though this exponential term might initially seem discouraging, we set  $D = 3$  in our experiments and observe no significant improvements for larger  $D$ . This is also consistent with findings from distributional RL (Bellemare et al., 2017), where a surprisingly small number of bins/quantiles are sufficient for state of the art performance on Atari games.

## 4. Asymptotic Convergence

In this section we prove some asymptotic convergence and regret guarantees for GLCB. More concretely, we state that the representation error can be made arbitrarily small by a sufficiently large GLN, and prove that the estimation and policy errors tends to zero for  $t \rightarrow \infty$ . In this work we provide only asymptotic results, which should be interpreted as a basic sanity check of our method and a starting point for further analysis; the main justification for our approach is the empirical performance which we explore later.

Note that we were only able to prove convergence for min-pseudocounts  $\text{AGG} = \min$  (2), while we found empirically that median-pseudocounts worked better in practice.

For the rest of this section, we assume that the pseudocount used in GLCB of total signature  $s$  for action  $a$  is defined as

$$\widehat{N}_t(s, a) := \min_{u \in \mathcal{U}} N_t(s_u, a)$$

which is sandwiched between

$$N_t(s, a) \leq \widehat{N}_t(s, a) \leq N_t(s_u, a) \quad \forall u$$

which further motivates the term 'pseudocount'. The first inequality follows from  $N_t(s, a) \leq N_t(s_u, a) \quad \forall u$  since condition  $g(x) = s$  is stronger than  $g_u(x) = s_u$ .

We first need to show that every action  $a$  is taken infinitely often in every observed context  $s_u$ , for every unit  $u$ :

**Lemma 1 (action lemma)** For  $s \in \mathcal{S}^U$ , if  $N_t(s) \rightarrow \infty$ , then  $N_t(s_u, a) \rightarrow \infty \quad \forall u \in \mathcal{U} \quad \forall a \in \mathcal{A}$ .

*Proof.* Fix some  $s$  for which the assumption  $N_t(s) \rightarrow \infty$  is satisfied. That is,  $s_t := g(x_t)$  equals  $s$  infinitely often. Yet another way of expressing this is that set  $\mathcal{T} := \{t \in \mathbb{N} : s_t = s\}$  is infinite.

Assume there is a set of actions  $\mathcal{A}_0 \subseteq \mathcal{A}$  for which the pseudocount in signature  $s$  is bounded, i.e.  $\mathcal{A}_0 = \{a : \widehat{N}_t(s, a) \not\rightarrow \infty\}$ , which implies there exist finite  $c_a$  and  $t_a$  for which

$$\widehat{N}_t(s, a) = c_a < \infty \quad \forall t \geq t_a \quad \forall a \in \mathcal{A}_0$$

We will show that this leads to a contradiction. Assume  $t \in \mathcal{T}$  and  $t \geq t_a \quad \forall a \in \mathcal{A}_0$ . Then for  $a \in \mathcal{A}_0$  we have

$$\text{GLNUB}_a^{\bar{t}}(x_t) \geq r_{\min} + C \sqrt{\frac{\log t}{\widehat{N}_{\bar{t}}(s_t, a)}} = C \sqrt{\frac{\log t}{c_a}}$$

since  $\text{GLN}_a^{\bar{t}}(x) \geq r_{\min}$ , and  $s_t = s$ . On the other hand, for  $t \in \mathcal{T}$  and  $a \notin \mathcal{A}_0$  we have  $\widehat{N}_{\bar{t}}(s, a) \rightarrow \infty$ , which implies

$$\text{GLNUB}_a^{\bar{t}}(x_t) \leq r_{\max} + C \sqrt{\frac{\log t}{\widehat{N}_{\bar{t}}(s, a)}} = o(\sqrt{\log t})$$

since  $\text{GLN}_a^{\bar{t}}(x) \leq r_{\max}$ . Both bounds together imply that for sufficiently large  $t \in \mathcal{T}$ ,

$$\text{GLNUB}_{a_0}^{\bar{t}}(x_t) > \text{GLNUB}_{a_1}^{\bar{t}}(x_t) \quad \forall a_0 \in \mathcal{A}_0 \quad \forall a_1 \notin \mathcal{A}_0$$

Hence for such a  $t$ , GLCB takes *some* action  $a_0 \in \mathcal{A}_0$ , leading to a contradiction  $\widehat{N}_t(s, a_0) \geq c_{a_0} + 1$ . Therefore, the assumption  $a_0 \in \mathcal{A}_0$  was wrong, and by induction  $\mathcal{A}_0 = \{\}$ , hence  $\widehat{N}_t(s, a) \rightarrow \infty \quad \forall a \in \mathcal{A}$ , which implies  $N_t(s_u, a) \rightarrow \infty \quad \forall u \in \mathcal{U}$ . This last step relies on

AGG=min. ■

Next we need that the GLN online learning Algorithm 1 converges, *assuming* every signature is observed infinitely often:

**Proposition 2 (convergence of GLN)** *Let  $a \in \mathcal{A}$  and  $x \in \mathcal{X}$ . Then the estimation error  $EstErr(x) := \text{GLN}_a^{\bar{t}}(x) - \text{GLN}_a^\infty(x) \rightarrow 0$  w.p.1. for  $t \rightarrow \infty$  if  $N_t(s_u, a) \rightarrow \infty \forall u \in \mathcal{U}$  w.p.1, where  $s_u := g_u(x)$ .*

The Proposition as stated (only) establishes that the limit exists. Roughly, on-average within each context cell  $g_u^{-1}(s_u)$ ,  $\text{GLN}_a^\infty$  is equal to the true expected reward, which by Theorem 6 below implies that in a sufficiently large GLN,  $\text{GLN}_a^\infty(x)$  is arbitrarily close to the true expected reward  $\mathbb{E}[r|x, a]$ .

*Proof sketch.* The condition means, every signature appears infinitely often for each unit  $u$ , which suffices for GLN to converge. For the first layer, this essentially follows from the convergence of SGD on i.i.d. data. Since the weights of layer 1 converge, the inputs to the higher GLN layers are asymptotically i.i.d., and a similar analysis applies to the higher layers. See (Veness et al., 2017, Thm.1) for details and proof. ■

The next theorem shows that GLCB Algorithm 2 converges to the correct value for all total signatures that have non-zero probability:

**Theorem 3 (convergence of GLCB)** *For any finite or continuous  $\mathcal{X} \ni x$ ,  $EstErr(x) := \text{GLN}_a^{\bar{t}}(x) - \text{GLN}_a^\infty(x) \rightarrow 0$  w.p.1 for  $t \rightarrow \infty$  for all  $a \in \mathcal{A}$  and  $\forall x : P(\mathbf{s}) > 0$ , where  $\mathbf{s} := \mathbf{g}(x)$ .*

*Proof.* By assumption,  $x_1, \dots, x_t$  are sampled i.i.d. from probability measure  $P$  with  $x \in \mathcal{X}$ , where  $\mathcal{X}$  may be discrete or continuous ( $\mathcal{X} \subseteq [0; 1]^d$  in the experiments). Then  $P(\mathbf{s}) := P[\mathbf{g}(x) = \mathbf{s}]$  is a discrete probability (mass function) over finite space  $\mathcal{S}^U \ni \mathbf{s}$ . Note that  $P(\mathbf{s}) = 0$  implies  $N_t(\mathbf{s}) = 0$ , hence such  $\mathbf{s}$  can safely be ignored. Consider  $P(\mathbf{s}) > 0$ , which implies  $N_t(\mathbf{s}) \rightarrow \infty$  for  $t \rightarrow \infty$  w.p.1, indeed,  $N_t(\mathbf{s})$  grows linearly w.p.1. By Lemma 1, this implies  $N_t(s_u, a) \rightarrow \infty \forall u \in \mathcal{U} \forall a \in \mathcal{A}$  w.p.1. By Proposition 2, this implies  $\text{GLN}_a^{\bar{t}}(x) \rightarrow \text{GLN}_a^\infty(x)$  w.p.1  $\forall a$ . ■

In the realizable case in which  $\text{GLN}_a^\infty(x)$  can represent the expected reward  $Q(x, a)$  exactly, the asymptotic GLCB policy

$$\tilde{\pi}(x) \in \tilde{\Pi}(x) := \arg \max_a \text{GLN}_a^\infty(x)$$

is (Bayes) optimal. In the unrealizable case, which we consider here,  $\tilde{\pi}$  is only the “optimal” *realizable* policy. The

resulting estimation error will be defined and taken into account later. The next lemma shows that sub-“optimal” (w.r.t.  $\tilde{\pi}$ ) actions are taken sublinearly often.

**Lemma 4 (sub-optimal action lemma)** *Sub-“optimal” actions are taken with vanishing frequency. Formally,  $N_t(\mathbf{s}, a) = o(t)$  w.p.1  $\forall a \notin \tilde{\Pi}(x)$ , where  $\mathbf{s} = \mathbf{g}(x)$ .*

*Proof.* Since  $P(\mathbf{s}) = 0$  trivially implies  $N_t(\mathbf{s}, a) = 0$ , we can assume  $P(\mathbf{s}) > 0$ . Assume  $N_t(\mathbf{s}, a)$  grows faster than  $\log t$ . Then

$$\sqrt{\frac{\log t}{\widehat{N}_t(\mathbf{s}_t, a_t)}} \leq \sqrt{\frac{\log t}{N_t(\mathbf{s}_t, a_t)}} \xrightarrow{w.p.1} 0 \text{ for } t \rightarrow \infty \quad (3)$$

This step uses  $\widehat{N}_t \geq N_t$ , which is true for all 3 choices of AGG (2). This implies  $\text{GLNUB}_a^{\bar{t}} \rightarrow \text{GLN}_a^\infty < \max_a \text{GLN}_a^\infty \leftarrow \max_a \text{GLN}_a^{\bar{t}} \leq \max_a \text{GLNUB}_a^{\bar{t}}$ . The convergence for  $t \rightarrow \infty$  w.p.1 follows from (3) and Theorem 3. The inequality is strict for sub-“optimal”  $a$ . Hence GLCB does not take action  $a \notin \tilde{\Pi}(x)$  anymore for large  $t$ , which contradicts  $N_t(s_u, a) \rightarrow \infty$ . ■

Let us now turn to the regret, that is the error measured in terms of lost reward suffered by the online learning GLN policy  $\pi_t$  compared to the “optimal” realizable policy  $\tilde{\pi}$  in hindsight:

**Theorem 5 (pseudo-regret / policy error)** *Let  $PolErr(x) := \text{GLN}_{\tilde{\pi}(x)}^\infty(x) - \text{GLN}_{\pi_t(x)}^\infty(x)$  be the simple regret incurred by the GLCB (learning) policy  $\pi_t(x)$ . Then the total pseudo-regret*

$$Regret(x_{1:T}) := \sum_{t=1}^T PolErr(x_t) = o(T) \text{ w.p.1}$$

*which implies  $PolErr(x) \rightarrow 0$  in Cesaro average.*

*Proof.*

$$\begin{aligned} Regret(x_{1:T}) &:= \sum_{t: a_t \notin \tilde{\Pi}(x_t)} PolErr(x_t) \\ &\leq r_{max} \sum_{\mathbf{s} \in \mathcal{S}^U} \#\{(x_t, a_t) : a_t \notin \tilde{\Pi}(x_t) \wedge \mathbf{g}(x_t) = \mathbf{s}\} \\ &\leq r_{max} \max_{x: \mathbf{g}(x) = \mathbf{s}} \sum_{\mathbf{s} \in \mathcal{S}^U} \sum_{a \notin \tilde{\Pi}(x)} N_T(\mathbf{s}, a) = o(T) \end{aligned}$$

The last equality follows from Lemma 4. ■

Typically the GLN cannot represent the true expected reward exactly, which will introduce a (small) representation error (also known as approximation error):

**Theorem 6 (representation error)** *Let  $Q(x, a) := \mathbb{E}[r|x, a] = P[r = 1|x, a]$  be the true expected reward*

of action  $a$  in context  $x$ . Let  $\pi^*(x) := \arg \max_a Q(x, a)$  be the (Bayes) optimal policy (in hindsight). Then, for Lipschitz  $Q$  and sufficiently large GLN,  $Q$  can be represented arbitrarily well, i.e. the (asymptotic) representation error (also known as approximation error)  $RepErr(x) := \max_a |Q(x, a) - GLN_a^\infty(x)|$  can be made arbitrarily small.

The Theorem is stated for Bernoulli rewards, but also holds for bounded continuous rewards if GLN is replaced by CTREE. *Proof.* Follows from (Veness et al., 2017, Thm.14) in the Bernoulli case, and similarly for CTREE, since the reward distribution and hence expected reward can be approximated arbitrarily well for sufficiently large tree depth  $D$ . ■

Finally we can connect the dots and bound the true regret in terms of policy and representation error:

**Corollary 7 (Simple Q-regret)**

$$Q(x, \pi^*(x)) - Q(x, \pi_t(x)) \leq PolErr(x) + 2RepErr(x)$$

*Proof.* Follows from

$$\begin{aligned} Q(x, \pi^*(x)) &= \max_a Q(x, a) \\ &\leq RepErr(x) + \max_a GLN_a^\infty(x) \\ &= RepErr(x) + GLN_{\pi^*(x)}^\infty(x), \text{ and} \\ Q(x, a) &\geq GLN_a^\infty(x) - RepErr(x) \end{aligned}$$

and the definition of  $PolErr(x)$  in Theorem 5. ■

Corollary 7 shows that the simple regret of GLCB is bounded by twice the representation error (which by Thm. 3 can be made small by a large GLN) and the policy error (which by Thm. 6 tends to zero in Cesaro average).

Providing finite time guarantees would obviously be a desirable next step, though in our case the situation is considerably complicated by the necessity of having to account for the cascading effects of having essentially a network of on-line learning algorithms running into parallel. In some sense this is the price we pay for the richness of the GLN model class. That said, what we can say theoretically is stronger than what one can say about typical deep contextual bandit algorithms, whose justification is almost entirely empirical.

**5. Experiments**

We evaluate GLCB against 9 state-of-the-art bandit algorithms, as implemented in the ‘‘Deep Bayesian Bandits’’ library (Riquelme et al., 2018), which we describe further in the Appendix. Each uses a neural network to estimate action values from a context, and selects actions greedily or

Environment	$ \mathcal{D} $	$ \mathcal{A} $	$d$	rewards
adult	45k	14	94	{0, 1}
census	2.5M	9	389	{0, 1}
covertime	581k	7	54	{0, 1}
financial	3.7k	8	21	{0, 1}
jester	19k	8	32	[0, 1]
statlog	43.5k	7	9	[0, 1]
wheel	-	5	2	[0, 10]

Table 1. Summary of all considered bandit tasks. Note that the *wheel* environment is synthetically generated, therefore the size of the context set is not given.

Algorithm	adult	census	covertime	statlog	financial	jester	wheel	median rank	mean rank
GLCB (ours)	<b>1</b>	<b>1</b>	7	<b>1</b>	3	<b>1</b>	2	<b>1</b>	2.1
BootRMS	2	2	<b>1</b>	3	4	2	8	2	3.0
Dropout	3	3	4	6	6	3	5	4	4.3
LinFullPost	5	8	5	5	<b>1</b>	6	<b>1</b>	5	4.5
NeuralLinear	7	5	6	2	2	7	3	5	4.6
NeuralGreedy	4	4	3	7	5	4	9	4	5.0
BBB	6	7	2	4	8	5	6	6	5.5
ParamNoise	8	6	8	8	7	10	4	8	7.4
constSGD	9	9	9	9	9	8	6	9	8.5
BBAlphaDiv	10	10	10	10	10	9	10	10	9.9

Table 2. Ranks of bandit algorithms based on average cumulative rewards obtained per dataset, sorted by mean.

via Thompson sampling. The neural networks themselves are trained using batch SGD with respect to the set of previously observed contexts. Importantly and in contrast, GLCB is online and does not require looping over or storing previous data. We use the implementation and hyperparameters provided by (Riquelme et al., 2018), and found that further parameter tuning yielded negligible improvement. We tune two sets of parameters for GLCB using grid search, one for the set of Bernoulli bandit tasks and another for the set of continuous bandit tasks, which we report in the appendix.

Each algorithm is evaluated using seven of the ten contextual bandit problems described in (Riquelme et al., 2018) – four discrete tasks (*adult*, *census*, *covertime* and *statlog*) adapted from classification problems, and three continuous tasks adapted from regression problems (*financial*, *jester* and *wheel*). The three dropped tasks were either trivial or did not fit the 0/1 Bernoulli or continuous bandit formulation. A summary of each task is provided in Table 1. For each time step  $t$ , a context  $x \in \mathcal{D}$  is sampled without replacement until  $t = T = \min\{5000, |\mathcal{D}|\}$  (e.g. the *financial* task run for only  $|\mathcal{D}| = 3713$  steps).

Table 2 presents the performance of GLCB compared to nine



state-of-the-art contextual bandits algorithms. Note that GLCB is the only algorithm that is online, as discussed earlier. It is evident that GLCB performs well on both discrete and continuous bandit problems, obtaining the best average rank across the seven tasks considered. Note that these results utilize median-aggregation for the GLCB policy, which we found to perform similarly to mean-aggregation. This is demonstrated in the Appendix. By comparison, we find that min-aggregation fails to generalize (pseudo counts remain close to 0) despite its desirable theoretical properties.

## 6. Discussion

We have introduced a new algorithm for both the discrete and continuous contextual bandits setting. Leveraging architectural properties of the recently-proposed Gated Linear Networks, we were able to efficiently estimate the uncertainty of our predictions with minimal computational overhead. Our GLCB algorithm outperforms all nine considered state-of-the-art contextual bandit algorithms across a standard benchmark of bandit problems, despite being the only considered algorithm that is online.

## References

- Auer, P., Cesa-Bianchi, N., and Fischer, P. Finite-time analysis of the multiarmed bandit problem. *Mach. Learn.*, 47(2-3):235–256, May 2002. ISSN 0885-6125. doi: 10.1023/A:1013689704352. URL <https://doi.org/10.1023/A:1013689704352>.
- Bellemare, M., Srinivasan, S., Ostrovski, G., Schaul, T., Saxton, D., and Munos, R. Unifying count-based exploration and intrinsic motivation. In Lee, D. D., Sugiyama, M., Luxburg, U. V., Guyon, I., and Garnett, R. (eds.), *Advances in Neural Information Processing Systems 29*, pp. 1471–1479. Curran Associates, Inc., 2016.
- Bellemare, M. G., Dabney, W., and Munos, R. A distributional perspective on reinforcement learning. In *Proceedings of the 34th International Conference on Machine Learning - Volume 70, ICML’17*, pp. 449–458. JMLR.org, 2017. URL <http://dl.acm.org/citation.cfm?id=3305381.3305428>.
- Blundell, C., Cornebise, J., Kavukcuoglu, K., and Wierstra, D. Weight uncertainty in neural network. In Bach, F. and Blei, D. (eds.), *Proceedings of the 32nd International Conference on Machine Learning*, volume 37 of *Proceedings of Machine Learning Research*, pp. 1613–1622, Lille, France, 07–09 Jul 2015. PMLR. URL <http://proceedings.mlr.press/v37/blundell15.html>.
- Charikar, M. S. Similarity estimation techniques from rounding algorithms. In *Proceedings of the Thiry-fourth Annual ACM Symposium on Theory of Computing*, STOC ’02, pp. 380–388, New York, NY, USA, 2002. ACM. ISBN 1-58113-495-9. doi: 10.1145/509907.509965. URL <http://doi.acm.org/10.1145/509907.509965>.
- Hernandez-Lobato, J., Li, Y., Rowland, M., Bui, T., Hernandez-Lobato, D., and Turner, R. Black-box alpha divergence minimization. In Balcan, M. F. and Weinberger, K. Q. (eds.), *Proceedings of The 33rd International Conference on Machine Learning*, volume 48 of *Proceedings of Machine Learning Research*, pp. 1511–1520, New York, New York, USA, 20–22 Jun 2016. PMLR. URL <http://proceedings.mlr.press/v48/hernandez-lobatob16.html>.
- Hinton, G. E. Training products of experts by minimizing contrastive divergence. *Neural Computation*, 14(8):1771–1800, August 2002.
- Kocsis, L. and Szepesvári, C. Bandit based Monte-Carlo planning. In *Proceedings of the 17th European Conference on Machine Learning, ECML’06*, pp. 282–293, Berlin, Heidelberg, 2006. Springer-Verlag. ISBN 3-540-45375-X, 978-3-540-45375-8. doi: 10.1007/11871842\_29. URL [http://dx.doi.org/10.1007/11871842\\_29](http://dx.doi.org/10.1007/11871842_29).
- Lattimore, T. and Hutter, M. Near-optimal PAC bounds for discounted MDPs. *Theoretical Computer Science*, 558: 125–143, 2014. ISSN 0304-3975. doi: 10.1016/j.tcs.2014.09.029.
- Lattimore, T. and Szepesvri, C. *Bandit Algorithms*. Cambridge University Press, 2020.
- Li, L., Chu, W., Langford, J., and Schapire, R. E. A contextual-bandit approach to personalized news article recommendation. In *Proceedings of the 19th International Conference on World Wide Web, WWW ’10*, pp. 661–670, New York, NY, USA, 2010. ACM. ISBN 978-1-60558-799-8. doi: 10.1145/1772690.1772758. URL <http://doi.acm.org/10.1145/1772690.1772758>.
- Mandt, S., Hoffman, M., and Blei, D. A variational analysis of stochastic gradient algorithms. In Balcan, M. F. and Weinberger, K. Q. (eds.), *Proceedings of The 33rd International Conference on Machine Learning*, volume 48 of *Proceedings of Machine Learning Research*, pp. 354–363, New York, New York, USA, 20–22 Jun 2016. PMLR. URL <http://proceedings.mlr.press/v48/mandt16.html>.
- Mattern, C. Mixing strategies in data compression. In *2012 Data Compression Conference, Snowbird, UT, USA, April 10-12*, pp. 337–346, 2012.

- Mattern, C. Linear and geometric mixtures - analysis. In *2013 Data Compression Conference, DCC 2013, Snowbird, UT, USA, March 20-22, 2013*, pp. 301–310, 2013.
- Osband, I., Blundell, C., Pritzel, A., and Van Roy, B. Deep exploration via bootstrapped DQN. In Lee, D. D., Sugiyama, M., Luxburg, U. V., Guyon, I., and Garnett, R. (eds.), *Advances in Neural Information Processing Systems 29*, pp. 4026–4034. Curran Associates, Inc., 2016.
- Osband, I., Aslanides, J., and Cassirer, A. Randomized prior functions for deep reinforcement learning. In *Proceedings of the 32Nd International Conference on Neural Information Processing Systems, NIPS’18*, pp. 8626–8638, USA, 2018. Curran Associates Inc. URL <http://dl.acm.org/citation.cfm?id=3327757.3327952>.
- Plappert, M., Houthoofd, R., Dhariwal, P., Sidor, S., Chen, R. Y., Chen, X., Asfour, T., Abbeel, P., and Andrychowicz, M. Parameter space noise for exploration. In *International Conference on Learning Representations*, 2018. URL <https://openreview.net/forum?id=ByBA12eAZ>.
- Riquelme, C., Tucker, G., and Snoek, J. Deep Bayesian bandits showdown: An empirical comparison of Bayesian deep networks for Thompson sampling. In *International Conference on Learning Representations*, 2018. URL <https://openreview.net/forum?id=SyYe6k-CW>.
- Snoek, J., Rippel, O., Swersky, K., Kiros, R., Satish, N., Sundaram, N., Patwary, M. M. A., Prabhat, P., and Adams, R. P. Scalable Bayesian optimization using deep neural networks. In *Proceedings of the 32Nd International Conference on International Conference on Machine Learning - Volume 37, ICML’15*, pp. 2171–2180. JMLR.org, 2015. URL <http://dl.acm.org/citation.cfm?id=3045118.3045349>.
- Srivastava, N., Hinton, G., Krizhevsky, A., Sutskever, I., and Salakhutdinov, R. Dropout: A simple way to prevent neural networks from overfitting. *J. Mach. Learn. Res.*, 15(1):1929–1958, January 2014. ISSN 1532-4435. URL <http://dl.acm.org/citation.cfm?id=2627435.2670313>.
- Strehl, A. L. and Littman, M. L. An analysis of model-based interval estimation for Markov decision processes. *Journal of Computer and System Sciences*, 74(8):1309 – 1331, 2008. ISSN 0022-0000. doi: <https://doi.org/10.1016/j.jcss.2007.08.009>. URL <http://www.sciencedirect.com/science/article/pii/S0022000008000767>. Learning Theory 2005.
- Tang, H., Houthoofd, R., Foote, D., Stooke, A., Chen, X., Duan, Y., Schulman, J., De Turck, F., and Abbeel, P. #exploration: A study of count-based exploration for deep reinforcement learning. In *Proceedings of the 31st International Conference on Neural Information Processing Systems, NIPS’17*, pp. 2750–2759, USA, 2017. Curran Associates Inc. ISBN 978-1-5108-6096-4. URL <http://dl.acm.org/citation.cfm?id=3294996.3295035>.
- Veness, J., Bellemare, M. G., Hutter, M., Chua, A., and Desjardins, G. Compress and control. In *Proceedings of the Twenty-Ninth AAAI Conference on Artificial Intelligence, January 25-30, 2015, Austin, Texas, USA*, pp. 3016–3023, 2015. URL <http://www.aaai.org/ocs/index.php/AAAI/AAAI15/paper/view/9649>.
- Veness, J., Lattimore, T., Bhoopchand, A., Grabska-Barwinska, A., Mattern, C., and Toth, P. Online learning with gated linear networks. *CoRR*, abs/1712.01897, 2017. URL <http://arxiv.org/abs/1712.01897>.
- Veness, J., Lattimore, T., Bhoopchand, A., Budden, D., Mattern, C., Grabska-Barwinska, A., Toth, P., Schmitt, S., and Hutter, M. Gated linear networks, 2019.
- Zinkevich, M. Online convex programming and generalized infinitesimal gradient ascent. In *Machine Learning, Proceedings of the Twentieth International Conference (ICML 2003), August 21-24, 2003, Washington, DC, USA*, pp. 928–936, 2003.

---

## Appendix

---

**Experimental details.** We briefly describe the algorithms we used for benchmarking below. All of the methods store the data and perform mini-batch (neural network) updates to learn action values. All besides *Neural Greedy* quantify uncertainties around the expected action values and utilize Thompson sampling by drawing action value samples from posterior-like distributions.

- *Neural Greedy* estimates action-values with a neural network and follows  $\epsilon$ -greedy policy.
- *Neural Linear* utilizes a neural network to extract latent features, from which action values are estimated using Bayesian linear regression. Actions are selected by sampling weights from the posterior distribution, and maximizing action values greedily based on the sampled weights, similar to (Snoek et al., 2015).
- *Linear Full Posterior* (LINFULLPOST) performs a Bayesian linear regression on the contexts directly, without extracting features.
- *Bootstrapped Network* (BOOTRMS) trains a set of neural networks on different subsets of the dataset, similarly to (Osband et al., 2016). Values predicted by the neural networks form the posterior distribution.
- *Bayes By Backprop* (BBB) (Blundell et al., 2015) utilizes variational inference to estimate posterior neural network weights. BBBALPHADIV utilizes *Bayes By Backprop*, where the inference is achieved via expectation propagation (Hernandez-Lobato et al., 2016).
- *Dropout* policy treats the output of the neural network with dropout (Srivastava et al., 2014) – where each units output is zeroed with a certain probability – as a sample from the posterior distribution.
- *Parameter-Noise* (PARAMNOISE) (Plappert et al., 2018) obtains the posterior samples by injecting random noise into the neural network weights
- *Constant-SGD* (CONSTSGD) policy exploits the fact that stochastic gradient descent (SGD) with a constant learning rate is a stationary process after an initial “burn-in” period. The analysis in (Mandt et al., 2016) shows that, under some assumptions, weights at each gradient step can be interpreted as samples from a posterior distribution.

**Processing of datasets.** For GLCB we require contexts to be in  $[0, 1]$  and rewards to be in  $[a, b]$  for a known

$a$  and  $b$ . To achieve this for Bernoulli bandit tasks (*adult*, *census*, *covertype*, and *statlog*), let  $X$  be a  $T \times d$  matrix with each row corresponding to a dataset entry and each column corresponding to a feature. We linearly transform each column to the  $[0, 1]$  range, such that  $\min(X_{.j}) = 0$  and  $\max(X_{.j}) = 1$  for each  $j$ . Rescaling for the *jester*, *wheel* and *financial* tasks are trivial.

**Further Experimental Results.** We present the cumulative rewards used for obtaining the rankings (Table 2 of main text) in Table 3.

**Computing Infrastructure.** All computations are run on single-GPU machines.

**GLCB hyperparameters.** We sample the hyperplanes weights used in gating functions uniformly from a unit hypersphere, and biases from  $\mathcal{N}(d/2, \text{bias scale})$  i.i.d. where  $d$  is the context dimension. This term is needed to effectively transform context ranges from  $[0, 1]^d$  to  $[-1/2, 1/2]^d$ . We set the GLN weights such that for each unit the weights sum up to 1 and are equal. We decay the learning rate and the switching alpha of GLN via initial value/ $(1 + \text{decay rate} \times N_{t-1}(a))$  where  $N_{t-1}(a)$  is the number of times the given action is taken up until time  $t$ . We display the hyperparameters we use in the experiments in Table 4, most of which are chosen via grid search.

**List of Notation.** We provide a partial list of notation in Table 5, covering many of the variables introduced in Section 3 (Gated Linear Contextual Bandits) of the main text.

algorithm	adult	census	covertype	statlog	financial	jester	wheel
BBAAlphaDiv	18±2	932±12	1838±9	2731±15	1860±1	3112±4	1776±11
BBB	399±8	2258±12	2983±11	4576±10	2172±18	3199±4	2265±44
BootRMS	676±3	2693±3	<b>3002±7</b>	4583±11	2898±4	3269±4	1933±44
Dropout	652±5	2644±8	2899±7	4403±15	2769±4	3268±4	2383±48
GLCB	<b>678±5</b>	<b>2718±3</b>	2715±12	<b>4863±1</b>	3038±3	<b>3298±3</b>	4432±11
LinFullPost	463±2	1898±2	2821±6	4457±2	<b>3122±1</b>	3193±4	<b>4491±15</b>
NeuralGreedy	598±5	2604±14	2923±8	4392±17	2857±5	3266±8	1863±44
NeuralLinear	391±2	2418±2	2791±6	4762±2	3059±2	3169±4	4285±18
ParamNoise	273±3	2284±5	2493±5	4098±10	2224±2	3084±4	3443±20
constSGD	107±3	1399±22	1991±9	3896±18	1862±1	3136±4	2265±31

Table 3. Cumulative rewards averaged over 500 random environment seeds. Best performing policies per task are shown in bold. ± term is the standard error of the mean.

Hyperparameter	Bernoulli bandits	Continuous bandits	Symbol
GLN network shape	[1000, 100, 1]	[1000, 100, 1]	-
number of hyperplanes per unit	8	2	-
UCB exploration bonus	0.01	1	C
bias scale	0.01	0.05	-
aggregation function	median	median	AGG
initial learning rate	0.1	1	-
learning rate decay parameter	0.1	0.01	-
initial switching rate	10	1	-
switching rate decay parameter	1	0.1	-
tree depth	-	3	D

Table 4. GLCB hyperparameters used for the experiments.

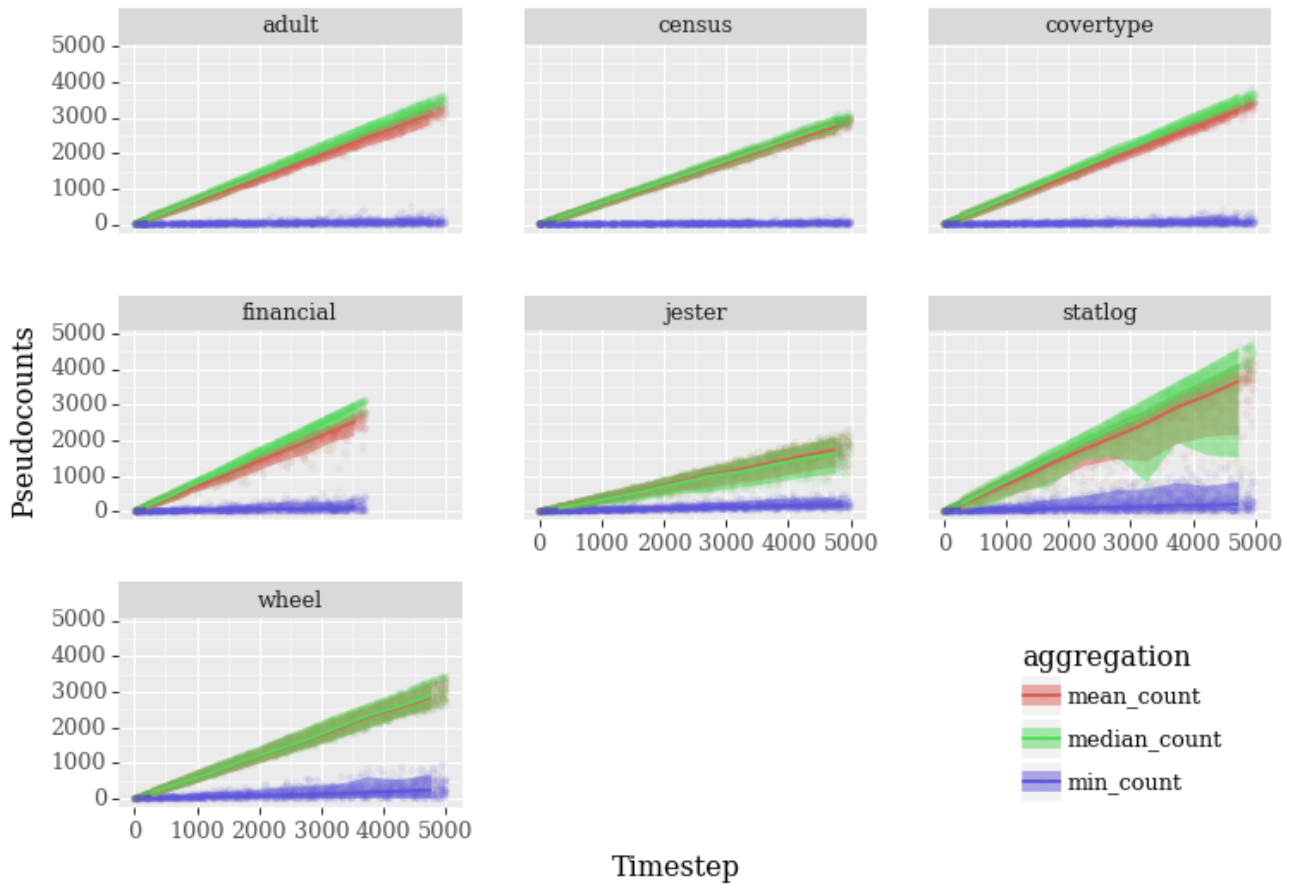


Figure 3. Growth of pseudocounts. We display the pseudocounts for the 0th action, for a fixed policy always choosing the 0th action. x-axis is the timestep and the y-axis is the pseudocount. The figures are obtained by running GLCB on 200 random environment seeds, recording pseudocounts derived from min, median, and mean, then subsampling  $10k$  time points. The plot lines are obtained via median smoothing, and the error bars/fillings are obtained such that 90% of the data is covered. Because all contexts are sampled without replacement, the actual state-context counts would remain constant at zero. We see that gating-based pseudocounts are able to generalize.

Symbol	Explanation
$K_0 - 1$	Dimension of a context
$\mathcal{X} \subseteq [0; 1]^{K_0 - 1}$	A context set
$x \in \mathcal{X}$	A context
$a \in \mathcal{A}$	Action from finite set of actions
$Q(x, a)$	True action value = expected reward of action $a$ in context $x$
$\varepsilon \in (0, 1/2)$	GLN output clipping parameter
$\epsilon$	Empty string
$\Theta_a^t$	Parameters of $\text{GLN}_a^t$
$\text{GLN}(x \Theta_a^t) \in [\varepsilon, 1 - \varepsilon]$	GLN used for estimating the reward probability of action $a$ at time $t$
$\text{GLN}_a^t : \mathcal{X} \rightarrow [\varepsilon, 1 - \varepsilon]$	Equivalent to $\text{GLN}(x \Theta_a^t)$ .
$U \in \mathbb{N}$	Number of GLN units
$\mathcal{U} = \{1, 2, \dots, U\}$	Index set for GLN units or gating functions
$u = (i, j) \in \mathcal{U}$	Index of gating function or GLN unit/neuron $j$ in layer $i$
$S$	Number of signatures
$\mathcal{S} = \{1, 2, 3, \dots, S\}$	Signature space of a gating function
$s_u \in \mathcal{S}$	Signature of unit $u$
$\mathbf{s} \in \mathcal{S}^U$	Total signature of all units $\mathcal{U}$
$g_u : \mathcal{X} \rightarrow \mathcal{S}$	Gating function for unit $u$ of $\text{GLN}_a$ for all $a$
$\mathbf{g} : \mathcal{X} \rightarrow \mathcal{S}^U$	Gating function applied element-wise to all $\mathcal{U}$
$\tau/t/T \in \mathbb{N}$	Some/current/maximum time step/index
$\top$	Boolean value for True
$\bar{t} \in \mathbb{N}$	$\bar{t} \equiv t - 1$
$x_{<t} \in \mathcal{X}^{t-1}$	Set of observed contexts that are observed up until time $\bar{t}$
$N_{\bar{t}}(s_u, a)$	Number of times $u$ th unit had signature $s_u$ given past contexts $x_{<t}$
$\widehat{N}_{\bar{t}}(\mathbf{g}(x), a)$	Pseudocount of $(x, a)$ at time $\bar{t}$ , calculated from $x_{<t}$
$C \in \mathbb{R}_{>0}$	UCB-like exploration constant
$\text{AGG} : \mathbb{N}^U \rightarrow \mathbb{R}_{\geq 0}$	An aggregation function such as min or mean or median
$r_{xat} \in \{0, 1\}$	Binary reward of action $a$ at context $x$ at time $t$
$\theta_{xa} \in [0, 1]$	Reward probability of action $a$ at context $x$
$[r_{\min}, r_{\max}]$	Range of continuous rewards
$D$	Depth of decision tree
$v$	Vector of midpoints of the leaf bins
$\mathcal{B} = \{0, 1\}$	Binary alphabet
$\mathcal{B}^{\leq D} / \mathcal{B}^{< D} / \mathcal{B}^D$	All/interior/leaf nodes of a tree
$b_{1:D}$	Indicator for a leaf node/bin
$P(b_{1:D} x)$	Probability of $x$ belonging to leaf $b_{1:D}$

Table 5. A (partial) list of variables used in the paper and their explanations.